

RESEARCH ARTICLE

Application of the Elitist-Mutated PSO and an Improved GSA to Estimate Parameters of Linear and Nonlinear Muskingum Flood Routing Models

Ling Kang[☉], Song Zhang^{*☉}

School of Hydropower and Information Engineering, Huazhong University of Science and Technology, Wuhan, China

☉ These authors contributed equally to this work.

* zhangs@hust.edu.cn



CrossMark
click for updates

OPEN ACCESS

Citation: Kang L, Zhang S (2016) Application of the Elitist-Mutated PSO and an Improved GSA to Estimate Parameters of Linear and Nonlinear Muskingum Flood Routing Models. PLoS ONE 11(1): e0147338. doi:10.1371/journal.pone.0147338

Editor: Wen-Bo Du, Beihang University, CHINA

Received: September 16, 2015

Accepted: December 31, 2015

Published: January 19, 2016

Copyright: © 2016 Kang, Zhang. This is an open access article distributed under the terms of the [Creative Commons Attribution License](https://creativecommons.org/licenses/by/4.0/), which permits unrestricted use, distribution, and reproduction in any medium, provided the original author and source are credited.

Data Availability Statement: All relevant data are within the paper and its Supporting Information files.

Funding: This study was partly supported by the Hubei Support Plan of Science and Technology of China (No. 2015BCA291), and the Wuhan Planning Project of Science and Technology of China (No. 2014060101010062).

Competing Interests: The authors have declared that no competing interests exist.

Abstract

Heuristic search algorithms, which are characterized by faster convergence rates and can obtain better solutions than the traditional mathematical methods, are extensively used in engineering optimizations. In this paper, a newly developed elitist-mutated particle swarm optimization (EMPSO) technique and an improved gravitational search algorithm (IGSA) are successively applied to parameter estimation problems of Muskingum flood routing models. First, the global optimization performance of the EMPSO and IGSA are validated by nine standard benchmark functions. Then, to further analyse the applicability of the EMPSO and IGSA for various forms of Muskingum models, three typical structures are considered: the basic two-parameter linear Muskingum model (LMM), a three-parameter nonlinear Muskingum model (NLMM) and a four-parameter nonlinear Muskingum model which incorporates the lateral flow (NLMM-L). The problems are formulated as optimization procedures to minimize the sum of the squared deviations (SSQ) or the sum of the absolute deviations (SAD) between the observed and the estimated outflows. Comparative results of the selected numerical cases (Case 1–3) show that the EMPSO and IGSA not only rapidly converge but also obtain the same best optimal parameter vector in every run. The EMPSO and IGSA exhibit superior robustness and provide two efficient alternative approaches that can be confidently employed to estimate the parameters of both linear and nonlinear Muskingum models in engineering applications.

Introduction

Accurate forecasting of flood wave movement in natural river channels is extremely important for the real-time monitoring, alert and control of floods, which are effective non-engineering measures for preventing tremendous loss of lives and property. Two categories of approaches for flood routing exist: hydraulic and hydrologic methods [1]. The former routes flood by

numerically solving the famous Saint-Venant equations, which usually has strict requirements for the topographical data of the investigated stream channel (such as channel cross-section and roughness) and complicated computations [2]. Conversely, the latter is based on the continuity and empirical storage equations and is more widely used in engineering applications due to its simplicity. The Muskingum flood routing model, developed by McCarthy [3], is the most frequently applied hydrologic technique.

As is known to all, the precise estimation of parameters is the key point in applying the Muskingum method for real-time flood forecasting [4]. This problem is always formulated and solved by determining the values of Muskingum parameters using historical inflow-outflow hydrograph data based on a specified optimization criterion (i.e., optimization objective). During the past decades, two types of diverse techniques have been developed to deal with the problem: traditional mathematical methods and heuristic optimization algorithms. The mathematical methods include the least-squares method (LSM) [5], the Hooke-Jeeves (HJ) pattern search in conjunction with the linear regression (HJ+LR), the conjugate gradient (HJ+CG) or the Davidon-Fletcher-Powell (HJ+DFP) algorithms [6], the nonlinear least-squares regression (NONLR) [7], the Broyden-Fletcher-Goldfarb-Shanno algorithm (BFGS) [8] and the Nelder-Mead simplex (NMS) algorithm [9]. However, most mathematical methods mentioned above inevitably have some drawbacks, such as special derivation conditions, a time-consuming quality or initial parameter assumptions. Therefore, numerous researchers focus on heuristic optimization algorithms that are characterized by fast convergence and the ability to obtain better solutions in recent decades, such as the harmony search (HS) [10], the genetic algorithm (GA) [11], the standard, improved or hybrid particle swarm optimization algorithms (PSOs) [12–15], the immune clonal selection algorithm (ICSA) [16], the differential evolution (DE) [17], and the cuckoo search (CS) algorithm [18].

The purpose of this research is to apply the newly developed elitist-mutated PSO (EMPSO) algorithm [19] and an improved gravitational search algorithm (IGSA) to solve parameter estimation problems of different forms of Muskingum models (one linear structure and two nonlinear structures). The proposed IGSA is based on the gravitational search algorithm (GSA) [20]. These two improved algorithms both have no previous applications for such issues. In the IGSA, a modified velocity updating rule and the elite strategy are introduced to enhance the global search ability and accelerate the convergence speed of the basic GSA, respectively. The experimental results of 9 widely-used standard benchmark functions with diverse properties demonstrate the global optimization abilities of the EMPSO and IGSA. The application cases verify their validity and advantages in handling parameter estimation problems of both linear and nonlinear Muskingum models.

The remainder of this paper is organized as follows: In Sect. 2, we provide the structures and the flood routing procedures of three important linear and nonlinear Muskingum models, whose structure complexities increase with the number of parameters from two to four. In Sect. 3, we briefly describe the newly developed EMPSO and the IGSA presented in this study, and then they are tested on 9 minimization benchmark functions. In Sect. 4, the EMPSO and the IGSA are successfully applied in numerical cases (three typical flood events). The results and analysis are also presented in this section. We discuss some conclusions of our research work in Sect. 5.

Muskingum Models

In previous decades, various forms of Muskingum models have been investigated [5, 18, 21]. Three typical linear or nonlinear Muskingum models and their corresponding flood routing equations or procedures are briefly described in this section: the original two-parameter linear

Muskingum model (LMM) [3], a three-parameter nonlinear Muskingum model (NLMM) [5] and a four-parameter nonlinear Muskingum model that incorporates the lateral flow (NLMM-L) [18].

LMM

The original LMM, which is based on the basic hypothesis that the storage within a river reach is a weighted function of inflow and outflow rates, employs the following continuity and storage equations.

$$\frac{dS_t}{dt} = I_t - O_t \tag{1}$$

$$S_t = K[xI_t + (1 - x)O_t], \quad (\text{LMM}) \tag{2}$$

where S_t = channel storage at time t ; I_t and O_t = observed rates of inflow and outflow at time t , respectively; K = storage-time constant, which has a value that is similar to the flow travel time through the routing river reach; x = weighting factor, $x \in (0, 0.3]$ for stream channels and $x \in (0, 0.5]$ for reservoir storage. The finite difference solution for Eqs (1) and (2) and the flood routing procedure of LMM is given by Eqs (3)–(5).

$$\hat{O}_0 = O_0 \tag{3}$$

$$\hat{O}_t = C_0I_t + C_1I_{t-1} + C_2\hat{O}_{t-1}, \quad (t = 1, \dots, T) \tag{4}$$

$$C_0 + C_1 + C_2 = 1 \tag{5}$$

where \hat{O}_t = estimated outflow at time t ; T = total number of time intervals; C_0 , C_1 and C_2 = three coefficients of LMM. Note that the LMM is a two-parameter (C_0 , C_1) Muskingum model because $C_2 = 1 - C_0 - C_1$.

NLMM

However, the relationship between the channel storage S_t and the weighted flow $[xI_t + (1 - x)O_t]$ is not always and essentially linear in many river reaches; thus, the use of LMM may be inappropriate. Hence, an additional exponent parameter m was introduced to consider the effect of nonlinearity. The following form of nonlinear Muskingum model has been suggested [5].

$$S_t = K[xI_t + (1 - x)O_t]^m, \quad (\text{NLMM}) \tag{6}$$

As shown in Eq (6), the NLMM is a three-parameter (K , x and m) Muskingum model and the LMM is a particular form of NLMM with $m = 1$. The rate of outflow O_t can be calculated by rearranging Eq (6):

$$O_t = \left(\frac{1}{1 - x}\right) \left(\frac{S_t}{K}\right)^{1/m} - \left(\frac{x}{1 - x}\right) I_t \tag{7}$$

NLMM-L

The LMM and NLMM are frequently viewed and discussed in the literature. However, they all disregard the lateral flow along the investigated reach despite the fact that lateral flow exists

along many river reaches in actual flood events. Assuming that the lateral flow (Q_{lat}) linearly varies along a river reach and can be expressed as a ratio (α) of the inflow rate ($Q_{lat} = \alpha I$), O'Donnell [21] proposed another linear Muskingum model that consider lateral flow in 1985, it is expressed as Eqs (8) and (9).

$$\frac{dS_t}{dt} = I_t + Q_{lat,t} - O_t = (1 + \alpha)I_t - O_t \tag{8}$$

$$S_t = K[x(1 + \alpha)I_t + (1 - x)O_t], \quad (\text{LMM} - \text{L}) \tag{9}$$

Inspired by the above assumptions by O'Donnell [21], in 2014, Karahan and Gurarslan [18] proposed a new nonlinear Muskingum model that takes the lateral flow into consideration after the integration of continuity Eq (8) and the NLMM in Eq (6):

$$S_t = K[x(1 + \alpha)I_t + (1 - x)O_t]^m, \quad (\text{NLMM} - \text{L}) \tag{10}$$

As expressed in Eq (10), the NLMM-L is a four-parameter (K , x , m and α) Muskingum model. By rearranging Eq (10), the rate of outflow O_t can be calculated using Eq (11).

$$O_t = \left(\frac{1}{1 - x}\right) \left(\frac{S_t}{K}\right)^{1/m} - \left[\frac{x(1 + \alpha)}{1 - x}\right] I_t \tag{11}$$

Routing Procedures of the NLMM and NLMM-L

In contrast to the LMM, the flood routing procedures of nonlinear Muskingum models NLMM and NLMM-L are highly complex. The routing procedures for the NLMM and the NLMM-L can be standardized using the following steps [2, 8, 18]:

Step 1: Assume values of the Muskingum parameters (K , x and m for NLMM; K , x , m and α for NLMM-L).

Step 2: Calculate the storage amount (S_t) using Eq (6) for the NLMM and Eq (10) for the NLMM-L.

Step 3: After combining the continuity Eqs (1) and (8) with the corresponding outflow calculations in Eqs (7) and (11), the time rate of the storage change can be calculated using Eq (12) for the NLMM and Eq (13) for the NLMM-L.

$$\frac{\Delta S_t}{\Delta t} = I_t - O_t = -\left(\frac{1}{1 - x}\right) \left(\frac{S_t}{K}\right)^{1/m} + \left(\frac{1}{1 - x}\right) I_t \tag{12}$$

$$\frac{\Delta S_t}{\Delta t} = (1 + \alpha)I_t - O_t = -\left(\frac{1}{1 - x}\right) \left(\frac{S_t}{K}\right)^{1/m} + \left(\frac{1 + \alpha}{1 - x}\right) I_t \tag{13}$$

Step 4: Calculate the next storage using Eq (14), where Δt is assumed to represent the unit time.

$$S_{t+1} = S_t + \Delta S_t \tag{14}$$

Step 5: Calculate the next estimated outflow (\hat{O}_{t+1}) using Eq (15) for the NLMM and Eq (16) for the NLMM-L.

$$\hat{O}_{t+1} = \left(\frac{1}{1-x}\right) \left(\frac{S_{t+1}}{K}\right)^{1/m} - \left(\frac{x}{1-x}\right) I_t \tag{15}$$

$$\hat{O}_{t+1} = \left(\frac{1}{1-x}\right) \left(\frac{S_{t+1}}{K}\right)^{1/m} - \left[\frac{x(1+\alpha)}{1-x}\right] I_t \tag{16}$$

Note that Eqs (15) and (16) use the observed inflow at the previous time-point (I_t) instead of the observed inflow at the current time (I_{t+1}) compared with Eqs (7) and (11) because Eq (15) occasionally provides better estimated outflow (\hat{O}_{t+1}) as suggested and reported by [6, 8].

Step 6: Repeat Steps 2–5 for all time steps.

Two Improved Heuristic Algorithms

Elitist-mutated PSO

Standard PSO and Its Developments. The PSO algorithm, originally introduced by Kennedy and Eberhart [22], is a population-based stochastic search technique inspired by the social behavior of fish schooling or bird flocking. In PSO, each individual within the swarm is called as a particle and represents a candidate solution to the optimization problem. For a D -dimensional search space, assume that $X_i = (x_{i1}, x_{i2}, \dots, x_{iD})$ and $V_i = (v_{i1}, v_{i2}, \dots, v_{iD})$ denote the position vector and the velocity vector of the i th particle, respectively. The best previously visited position of the i th particle and the current global best position in the swarm are recorded as $pbest_i = (p_{i1}, p_{i2}, \dots, p_{iD})$ and $gbest = (p_{g1}, p_{g2}, \dots, p_{gD})$, respectively, where g is the index of the best particle in the swarm. During iterations, the swarm is manipulated according to the updating rules written as Eqs (17) and (18). Note that such process involves individual intelligence, i.e., the particles learn through their own experience (local search) and the experience of their peers (global search).

$$v_{id}^{n+1} = v_{id}^n + c_1 r_1 (p_{id}^n - x_{id}^n) + c_2 r_2 (p_{gd}^n - x_{id}^n) \tag{17}$$

$$x_{id}^{n+1} = x_{id}^n + v_{id}^{n+1} \tag{18}$$

where $d = 1, \dots, D$ represents the index for the decision variables; $i = 1, \dots, pop$ and pop = the number of particles in the swarm; n = iteration number; r_1 and r_2 = uniformly generated random numbers in $[0, 1]$; c_1 and c_2 = cognitive and social parameters, respectively, which are referred to as acceleration constants. In addition, the value of velocity v_{id}^n in each iteration should be limited within the range $[-v_{d,max}, v_{d,max}]$, where $v_{d,max} = v \times (x_d^u - x_d^l)$, $0.05 \leq v \leq 0.50$, x_d^u and x_d^l are the lower bound and upper bound of the dimension d .

Eqs (17) and (18) yield the standard PSO that may have shortcomings of premature convergence and poor control of its search capability. To overcome these drawbacks, extended studies and developments were reported [23–26]. Among which, two big variations focus on modifying the model coefficients as follows.

In 1988, Shi and Eberhart [26] introduced a linearly decreasing inertia weight parameter w^n into Eq (17) to balance the local search and the global search abilities, which are expressed as

Eqs (19) and (20)

$$v_{id}^{n+1} = w^n v_{id}^n + c_1 r_1 (p_{id}^n - x_{id}^n) + c_2 r_2 (p_{gd}^n - x_{id}^n) \tag{19}$$

$$w^n = w_{\max} - (w_{\max} - w_{\min}) \times \frac{n}{N} \tag{20}$$

where w_{\max} and w_{\min} = the initial and the final inertia weights, respectively; n = current iteration number; and N = maximum iterations.

In 1999, Clerc [23] introduced the constriction factor χ to control the changes in velocity and assure better convergence of the PSO, as shown in Eqs (21) and (22).

$$v_{id}^{n+1} = \chi [v_{id}^n + c_1 r_1 (p_{id}^n - x_{id}^n) + c_2 r_2 (p_{gd}^n - x_{id}^n)] \tag{21}$$

$$\chi = \frac{2}{|2 - \varphi - \sqrt{\varphi^2 - 4\varphi}|}, \text{ where } \varphi = c_1 + c_2, \varphi > 4 \tag{22}$$

Other developments on improving the performance of PSO fall into two categories [24]: (1) considering the population structure [25, 27] and (2) altering the interaction modes between each particle and its neighbors [24, 28–30].

Latest Velocity Updating Rule and Elitist Mutation Operator. A newly developed PSO, namely, elitist-mutated PSO (EMPSO), was proposed by Nagesh Kumar and Janga Reddy [19] for solving water resource problems. Two main improvements in the EMPSO algorithm are: (1) each particle calculates its velocity using the latest updating rule as shown in Eq (23), where χ is the constriction coefficient and w is the inertia weight; and (2) a new strategic mechanism called elitist mutation operator is introduced to enhance the diversity of the swarm and explore new regions in the whole search space. Pseudo-code of the EMPSO algorithm is presented in Fig 1, in which Fig 1a gives the implementation of the elitist mutation operator and Fig 1b describes the main steps involved in the EMPSO methodology.

$$v_{id}^{n+1} = \chi [w v_{id}^n + c_1 r_1 (p_{id}^n - x_{id}^n) + c_2 r_2 (p_{gd}^n - x_{id}^n)] \tag{23}$$

As illustrated in Fig 1a, in each iteration, the elitist mutation operator is performed on a pre-defined number (NM) of the worst fitness particles in the swarm. This process of random perturbation is described as follows: first, all particles are sorted in ascending order based on their fitness function and the index numbers for the respective particles are obtained (i.e. index of the sorted swarm is recorded in ASF[i], $i = 1, \dots, \text{pop}$); second, the elitist mutation is performed on the front NM worst particles (selected number of least ranked particles to be elitist-mutated) and the respective particle position vectors are replaced with the new mutated position vectors obtained after performing variable-wise mutation on the global best position vector (p_{em} is the mutation probability), whereas the velocity vectors of these particles are unvaried.

Improved GSA

Basic GSA. Based on the law of gravity and mass interactions, in 2009, Rashedi and Nezamabadi-pour [20] proposed a novel heuristic algorithm, namely, the gravitational search algorithm (GSA). For an optimization problem, the searcher agents in GSA are a collection of masses in which the values of the masses are proportional to their fitness functions. During the iterative process, the masses interact with each other according to Newtonian gravity and the laws of motion. A heavier mass has a higher attraction, which indicates greater efficiency

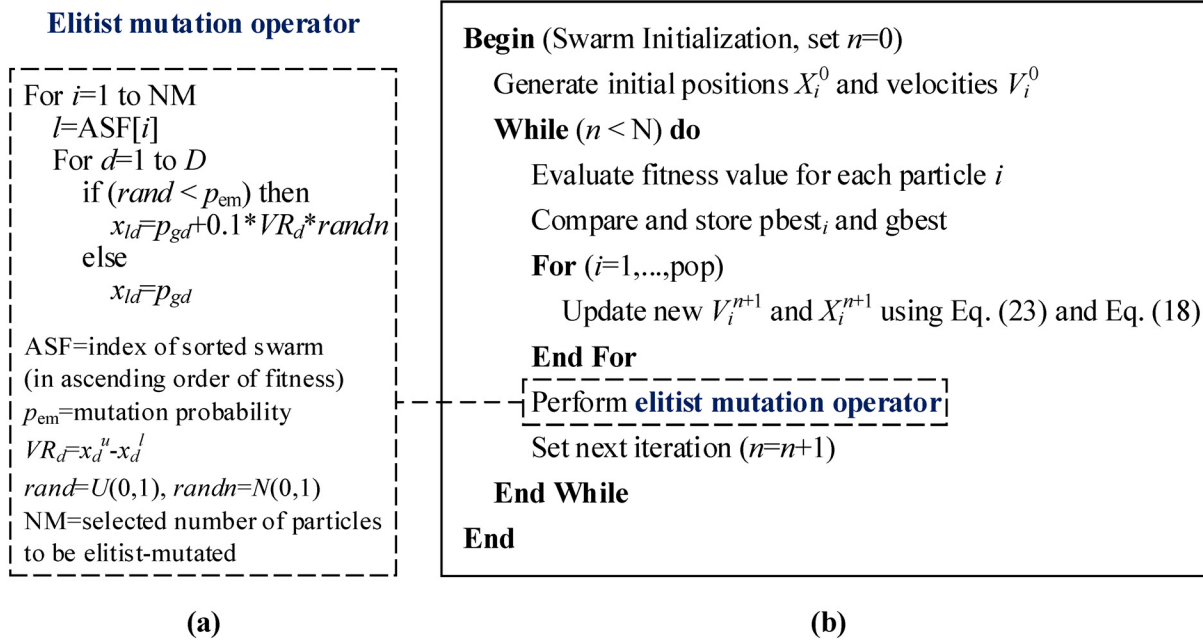


Fig 1. Pseudo-code of the EMPSO algorithm.

doi:10.1371/journal.pone.0147338.g001

(similar to the global optimum) and a slower speed of movement. The basic GSA is mathematically described as follows.

Consider a system with pop agents (masses), in which the position of the *i*th agent (candidate solution) is denoted by

$$X_i = (x_i^1, \dots, x_i^d, \dots, x_i^D) \quad \text{for } i = 1, \dots, \text{pop} \quad (24)$$

where x_i^d represents the position of the *i*th agent in the *d*th dimension and *D* is the space dimension. According to the Newton law of gravity, the force acting on the *i*th mass from the *j*th mass at time *t* is defined as Eq (25). The total force acting on agent *i* in the dimension *d* is considered to be a randomly weighted sum of the forces exerted from other agents, as expressed in Eq (26)

$$F_{ij}^d(t) = G(t) \frac{M_{pi}(t) \times M_{aj}(t)}{R_{ij}(t) + \epsilon} (x_j^d(t) - x_i^d(t)) \quad (25)$$

$$F_i^d(t) = \sum_{j \in Kbest, j \neq i} rand_j F_{ij}^d(t) \quad (26)$$

where M_{pi} , M_{aj} = the passive and active gravitational masses of agent *i* and agent *j*, respectively; $M_{ai} = M_{pi} = M_i$ $i = 1, \dots, \text{pop}$, M_i is the inertial mass of the *i*th agent; $G(t)$ = gravitational constant at time *t*; ϵ = a small constant; $R_{ij}(t) = \|X_i(t), X_j(t)\|_2$, is the Euclidian distance between agents *i* and *j*; $rand_j$ = a uniformly generated random number in [0, 1]; $Kbest$ = the set of first *K* agents with the best fitness values and the largest masses, which is a function of time *t*, has the initial value $K_0 = \text{pop}$ and is linearly decreases to 1 at the end of each iteration.

Note that the gravitational constant G is a function of the initial value (G_0 , a problem-dependent parameter) and time t :

$$G(t) = G(G_0, t) = G_0 \exp\left(-\beta \times \frac{t}{N}\right) \tag{27}$$

Based on the law of motion, the acceleration of the i th agent in the d th dimension at time t is given by

$$a_i^d(t) = \frac{F_i^d(t)}{M_i(t)} \tag{28}$$

The next velocity of each agent i is considered to be a fraction of its current velocity added to its acceleration and is expressed as follows:

$$v_i^d(t + 1) = rand_i \times v_i^d(t) + a_i^d(t) \tag{29}$$

$$x_i^d(t + 1) = x_i^d(t) + v_i^d(t + 1) \tag{30}$$

The inertia mass values of the masses are calculated by

$$m_i(t) = \frac{fit_i(t) - worst(t)}{best(t) - worst(t)} \text{ and } M_i(t) = \frac{m_i(t)}{\sum_{j=1}^N m_j(t)} \tag{31}$$

where $fit_i(t)$ = the fitness value of the agent i at time t ; $worst(t)$ and $best(t)$ = the worst fitness and the best fitness, respectively, among all agents.

Modified Velocity Updating Rule and Elite Strategy. The basic GSA may spend a significant amount of time converging to the global optimum due to the presence of heavier masses at the end of every run. Therefore, we propose an improved GSA (IGSA) which employs the following two strategies to overcome this drawback. The first strategy learns from the idea of memory and social information of PSO and defines a new velocity updating rule for agents, which is written as Eq (32) [31]. The second strategy adds the elite strategy to GSA to accelerate its convergence speed. The idea is to directly preserve a certain number of elite agents in the current generation and replace an equal number of worst agents of the new generated offspring generation. The top 5% of agents are preserved in each generation. Pseudo-code of the IGSA is shown in Fig 2.

$$v_i^d(t + 1) = rand_i \times v_i^d(t) + c_1 r_1 a_i^d(t) + c_2 r_2 (x_g^d(t) - x_i^d(t)) \tag{32}$$

where $rand_i$, r_1 and r_2 = uniformly generated random numbers in $[0, 1]$; c_1 and c_2 = weighting factors; and $x_g^d(t)$ = the current best solution.

Performance Test Using Benchmark Functions

Benchmark functions are commonly recognized as an important tool to validate the performance of optimization algorithms [24, 25, 32]. There have been many kinds of benchmark functions reported in the literature [33, 34]. However, only a comprehensive selection of benchmark functions with various characteristics can be truly useful to test new algorithms in an unbiased way. For this reason, a rich test suite of 9 standard minimization benchmark functions with diverse properties in terms of separability, modality were used as experiments for evaluating the EMPSO and IGSA. Table 1 gives a detailed description of these functions, where D is the dimension of the function, f_{min} is the optimum value of the function. Functions f1–f7 are high-dimensional problems. The first four functions (f1 to f4) are unimodal,

```

Begin
Population Initialization, set  $t=0$ 
While ( $t < N$ ) do
    Evaluate fitness  $fit_i(t)$  for each agent  $i$ 
    Elites preserving
    Update  $G(t)$ ,  $best(t)$  and  $worst(t)$  of the population
    Calculate  $M_i(t)$ ,  $F_i^d(t)$ , and  $a_i^d(t)$  for each agent  $i$ 
    For ( $i=1, \dots, pop$ )
        Update new velocity  $V_i(t)$  and position  $X_i(t)$  using Eq. (32) and Eq. (30)
    End For
    Elites replacement
    Set next iteration ( $t=t+1$ )
End While
End
    
```

Fig 2. Pseudo-code of the IGSA.

doi:10.1371/journal.pone.0147338.g002

Table 1. Benchmark functions.

No.	Formula	D	Range	f_{min}	Separability	Modality
f1	$f_1(X) = \sum_{i=1}^D x_i^2$	30	$[-100, 100]^D$	0	Separable	Unimodal
f2	$f_2(X) = \sum_{i=1}^D x_i + \prod_{i=1}^D x_i $	30	$[-10, 10]^D$	0	Non-Separable	Unimodal
f3	$f_3(X) = \sum_{i=1}^D \left(\sum_{j=1}^i x_j \right)^2$	30	$[-100, 100]^D$	0	Non-Separable	Unimodal
f4	$f_4(X) = \sum_{i=1}^{D-1} [100(x_{i+1} - x_i^2)^2 + (x_i - 1)^2]$	30	$[-30, 30]^D$	0	Non-Separable	Unimodal
f5	$f_5(X) = \sum_{i=1}^D -x_i \sin(\sqrt{ x_i })$	30	$[-500, 500]^D$	$-418.9829 \times D$	Separable	Multimodal
f6	$f_6(X) = -20 \exp\left(-0.2 \sqrt{\frac{1}{D} \sum_{i=1}^D x_i^2}\right) - \exp\left(\frac{1}{D} \sum_{i=1}^D \cos(2\pi x_i)\right) + 20 + e$	30	$[-32, 32]^D$	0	Non-Separable	Multimodal
f7	$f_7(X) = \frac{1}{4000} \sum_{i=1}^D x_i^2 - \prod_{j=1}^D \cos\left(\frac{x_j}{\sqrt{j}}\right) + 1$	30	$[-600, 600]^D$	0	Non-Separable	Multimodal
f8	$f_8(X) = \left(\frac{1}{500} + \sum_{j=1}^{25} \frac{1}{j + \sum_{i=1}^2 (x_i - a_j)^6} \right)^{-1}$	2	$[-65.536, 65.536]^D$	1	Non-Separable	Multimodal
f9	$f_9(X) = -\sum_{i=1}^{10} [(X - a_i)(X - a_i)^T + c_i]^{-1}$	4	$[0, 10]^D$	-10.5	Non-Separable	Multimodal

The values of a_{ij} in f8 are given in [S1 Table](#).

The vectors a_i and c_i in f9 are given in [S2 Table](#).

doi:10.1371/journal.pone.0147338.t001

which are relatively easy to solve. Functions f5–f9 are multimodal so that the algorithm really suffers from being premature. Functions f5–f7, where the number of local minima increases exponentially with the problem dimension, appear to be the most difficult class of optimization problems. Functions f8 and f9 are two low-dimensional functions which have only a few local minima. We applied the EMPSO and IGSA to the above 9 benchmark functions and compared the experimental results with those obtained by the standard PSO as well as basic GSA. The results are averaged over 50 independent runs and the best-so-far solution, mean and standard deviation of the best solution in each run are listed in Table 2. In all cases, population size is set to 50 (pop = 50) and maximum number of iterations is 1000 (N = 1000). For PSO and EMPSO, the acceleration constants are $c_1 = 1.0$ and $c_2 = 0.5$. Other parameters of the EMPSO use the following settings: constriction factor $\chi = 0.9$, inertia weight $w = 1.0$, mutation probability $p_{em} = 0.2$, and the size of the elitist-mutated particles $NM = 10$. For GSA and IGSA, $G_0 = 1.0$ and $\beta = 20.0$, whereas $c_1 = 0.5$ and $c_2 = 1.5$ for the IGSA.

Table 2. Minimization results of benchmark functions in Table 1.

Function	Statistics	PSO	EMPSO	GSA	IGSA
f1	Best	3.03E+03	9.46E-16	8.94E-18	1.43E-18
	Mean	7.45E+03	1.29E-05	1.98E-17	3.48E-18
	Std.	1.99E+03	8.8E-05	5.74E-18	9.70E-19
f2	Best	2.93E+01	1.73E-02	1.32E-08	5.43E-09
	Mean	8.40E+01	2.80E-01	2.30E-08	7.72E-09
	Std.	6.46E+01	2.12E-01	3.60E-09	1.33E-09
f3	Best	1.95E+04	7.97	5.77E+04	1.48E+02
	Mean	3.06E+04	7.13E+01	1.02E+05	2.54E+03
	Std.	5.98E+03	6.01E+01	2.95E+04	1.66E+03
f4	Best	1.81E+06	1.78E+01	2.57E+01	1.45E+01
	Mean	6.85E+06	6.76E+01	2.69E+01	4.96E+01
	Std.	3.17E+06	6.68E+01	5.29	4.21E+01
f5	Best	-9091.9	-11437.2	-4249.3	-9299.7
	Mean	-7273.4	-10205.5	-2907.9	-7604.1
	Std.	8.23E+02	4.51E+02	4.67E+02	6.26E+02
f6	Best	1.26E+01	9.31E-01	2.43E-09	1.07E-09
	Mean	1.45E+01	2.00	3.35E-09	8.45E-01
	Std.	1.05	4.79E-01	4.55E-10	1.27
f7	Best	3.43E+01	3.83E-14	1.25	4.72E-02
	Mean	6.86E+01	3.59E-02	4.10	1.61
	Std.	1.91E+01	4.38E-02	1.62	2.08
f8	Best	0.9980	0.9980	0.9980	0.9980
	Mean	0.9981	0.9980	3.4961	1.2553
	Std.	1.74E-04	3.33E-16	2.25	8.58E-01
f9	Best	-10.0931	-10.5364	-10.5364	-10.5364
	Mean	-6.6513	-5.5079	-9.3011	-10.5364
	Std.	1.53	3.58	2.83	8.88E-15

Best: best-so-far solution over 50 runs.

Mean: mean of the best solutions in 50 runs.

Std.: standard deviation of the best solutions in 50 runs.

doi:10.1371/journal.pone.0147338.t002

As can be seen from Table 2, the best results are indicated in bold font. Generally speaking, the EMPSO provides much better results than PSO for all the 9 benchmark functions according to the three statistics (Best, Mean and Std.). The IGSA can find better solutions than GSA for functions f1–f7 and it strikingly improves the robustness of GSA (smaller values of Std.) on all functions except for function f6. If comprehensively consider the values of Best and Std., the EMPSO performs the best on 5 functions (f1, f2, f4, f6, f9) and IGSA is the best on the other 4 functions (f3, f5, f7, f8). The results in Table 2 also show that EMPSO and IGSA have better global optimization abilities than the PSO and GSA in solving most of the 9 benchmark functions and can obtain similar solutions.

Numerical Cases

In the parameter optimization problems of Muskingum models, minimization of the sum of the squared deviations (SSQ) or the sum of the absolute deviations (SAD) between the observed and the estimated outflows is always adopted as the objective function f , defined as follows:

$$\text{Minimize : } f = \text{SSQ} = \sum_{t=1}^T [O_t - \hat{O}_t(P)]^2 \tag{33}$$

$$\text{Minimize : } f = \text{SAD} = \sum_{t=1}^T |O_t - \hat{O}_t(P)| \tag{34}$$

where O_t = observed outflow at time t ; $\hat{O}_t(P)$ = estimated outflow at time t by the Muskingum routing equation that is Eq (4) for the LMM, Eq (15) for the NLMM and Eq (16) for the NLMM-L; P = the parameter vector need to be calibrated, where $P = (C_0, C_1)$ in LMM, $P = (K, x, m)$ in NLMM, $P = (K, x, m, \alpha)$ in NLMM-L.

To evaluate the practicability of the EMPSO algorithm and the IGSA in engineering applications, we applied these two improved heuristic algorithms to seek the optimal parameter vector P for the three different Muskingum models and compared the results with those obtained by RGA and standard PSO, as well as the basic GSA. The optimal parameter vectors obtained in this study are also compared with the best existing solutions reported in previous literature. For the above five algorithms, the iterations proceed until the stopping criterion is satisfied, which is expressed as

$$|f_{\text{best}}(n) - f_{\text{best}}(n - 1)| \leq \delta \quad \text{or} \quad n \leq N \tag{35}$$

where n is the iteration number and N is the maximum number of iterations (set to 5000); $f_{\text{best}}(n)$ is the best value of f in the n th iteration and δ is convergence accuracy.

For the five algorithms in applications, the population size pop was set to 50 and they were implemented on a PC with a 32-bit Windows 7 operating system, 4 GB RAM and 2.93 GHz-core (TM) i3-based processor. Each algorithm was performed over 50 runs on the three Muskingum models for the numerical examples. In RGA, the tournament selection, simulated binary crossover (SBX) and polynomial mutation operators [35] are used; the crossover probability $p_c = 0.85$ and mutation probability $p_m = 0.05$; the distribution index for SBX is 10 and the distribution index for the mutation operator is 100. Parameter settings of the PSO, EMPSO, GSA and IGSA are the same with Sect. 3.

Case 1: Application to LMM

Flood Data from the South Canal of China in August 1961. A flood occurred in the south canal of China between the Linqing River and the Chenggou Bay in August 1961, in which the inflow and outflow hydrographs exhibit obvious linear characteristics [36], is employed as the numerical case for the LMM, where $\Delta t = 12h$ and $T = 28$. The search ranges for the two parameters in LMM are set to $C_0, C_1 \in (0.00, 0.50)$. One best existing solution according to the literature [11] is $C_0 = 0.4736, C_1 = 0.0301$ and $SAD = 141.225$, which is used as a reference.

Results and Analysis. For comparison, the statistical results (Best, Worst, Mean, and Std.) of the SAD, the model parameters, the iteration number and the CPU time for convergence (convergence accuracy δ) by the five algorithms (RGA, PSO, GSA, EMPSO, IGSA) are listed in Table 3: (1) with the exception of RGA, the other four algorithms find the same optimal solution ($SAD = 141.194; C_0 = 0.4729$ and $C_1 = 0.0317$) after 50 runs, which is better than the reference; however, only the GSA, EMPSO and IGSA can steadily converge to the same optimal solution for the LMM in every run (values of Std. for the SADs and the parameters are 0.0000E+00), whereas the optimal solutions obtained by the PSO are slightly fluctuate between different runs; (2) the GSA and IGSA require more time to converge than other three algorithms; (3) compared with GSA and IGSA, the EMPSO has a faster convergence speed (only requires 120 iterations and an average 0.0067s of CPU time for convergence in every run) and exhibits better stability (smallest values of Std.). The estimated outflow hydrograph by the LMM using the best parameter vector obtained in this study is shown in Fig 3. Fig 4 shows the comparison of the average convergence rate among the five algorithms on the LMM.

Table 3. Statistics of different algorithms performed on the LMM over 50 runs for the 1961 flood from the south canal of China.

Algorithms	Statistics	<i>f</i>			Convergence ($\delta = 0.001$)	
		SAD	C_0	C_1	Iterations	CPU (s)
RGA	Best	141.196	0.4729	0.0316	4367	0.3852
	Worst	141.301	0.4721	0.0327	4491	0.3977
	Mean	141.220	0.4731	0.0312	3260	0.2894
	Std.	2.1616E-02	4.8277E-04	1.0421E-03	992.01	8.6446E-02
PSO	Best	141.194	0.4729	0.0317	2784	0.0668
	Worst	141.208	0.4730	0.0315	1111	0.0277
	Mean	141.200	0.4729	0.0316	2431	0.0586
	Std.	3.1968E-03	7.0425E-05	1.4650E-04	1410.09	3.3789E-02
GSA	Best	141.194	0.4729	0.0317	2147	0.5549
	Worst	141.194	0.4729	0.0317	2813	0.7099
	Mean	141.194	0.4729	0.0317	2519	0.6291
	Std.	0.0000E+00	0.0000E+00	0.0000E+00	153.99	3.1552E-02
EMPSO	Best	141.194	0.4729	0.0317	50	0.0037
	Worst	141.194	0.4729	0.0317	165	0.0088
	Mean	141.194	0.4729	0.0317	120	0.0067
	Std.	0.0000E+00	0.0000E+00	0.0000E+00	23.54	1.1736E-03
IGSA	Best	141.194	0.4729	0.0317	1175	0.3817
	Worst	141.194	0.4729	0.0317	2053	0.6155
	Mean	141.194	0.4729	0.0317	1754	0.5420
	Std.	0.0000E+00	0.0000E+00	0.0000E+00	155.33	4.2196E-02

doi:10.1371/journal.pone.0147338.t003

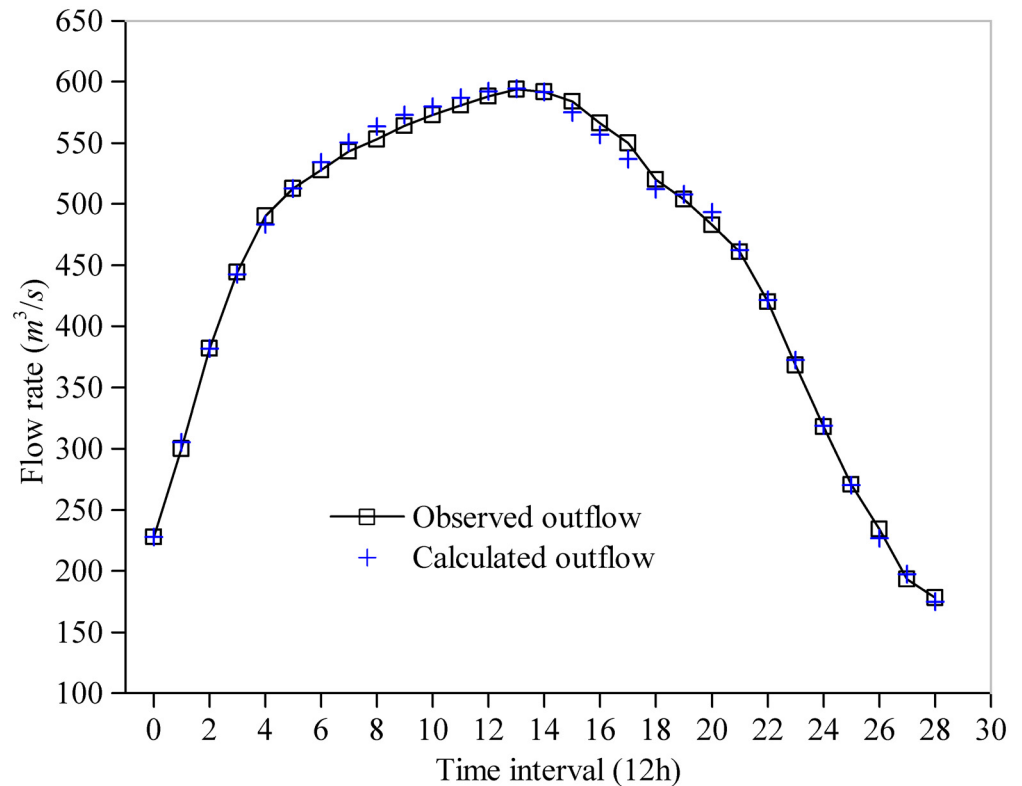


Fig 3. Fitting curve of outflow hydrograph of the LMM experiment.

doi:10.1371/journal.pone.0147338.g003

Case 2: Application to NLMM

Data Set of Wilson (1974). The data set from ref. [37], which had been demonstrated to have a nonlinear relationship between the storage and the weighted-flow [7], is taken as the numerical case for the NLMM. It is a single peak hydrograph that has been previously investigated by many researchers [2, 4, 7, 8, 10, 16–18, 21, 38], where $\Delta t = 6h$ and $T = 21$. The NLMM has three parameters and their search ranges are set to $K \in [0.01, 1.00]$, $x \in [0.00, 0.30]$ and $m \in [1.00, 3.00]$. One best existing solution for the NLMM refers to Xu and Qiu [17] using the differential evolution (DE) algorithm was $K = 0.5175$, $x = 0.2869$, $m = 1.8680$ and $SSQ = 36.77$.

Results and Analysis. The statistical results, which resemble Table 3, are also listed in Table 4: (1) only the EMPSO and IGSA can steadily converge to the same optimal solution ($SSQ = 36.7679$; $K = 0.5175$, $x = 0.2869$ and $m = 1.8680$) for the NLMM in every run, whereas optimal solutions obtained by RGA, PSO and GSA fluctuate between different runs; (2) for GSA, EMPSO and IGSA, the average number of iterations that are required for convergence in every run are approximately 2062, 191 and 780, respectively, and the corresponding CPU consuming times are 0.9992s, 0.0883s and 0.4864s; these data indicate that the EMPSO has a faster convergence speed and the IGSA obviously improves the convergence performance of GSA; (3) the EMPSO has the best performance in optimizing the NLMM (the lowest CPU time for every run and a steady fluctuation among of iterations with the lowest Std. = 51.22). The estimated outflow hydrograph by the NLMM using the best parameter vector obtained in this

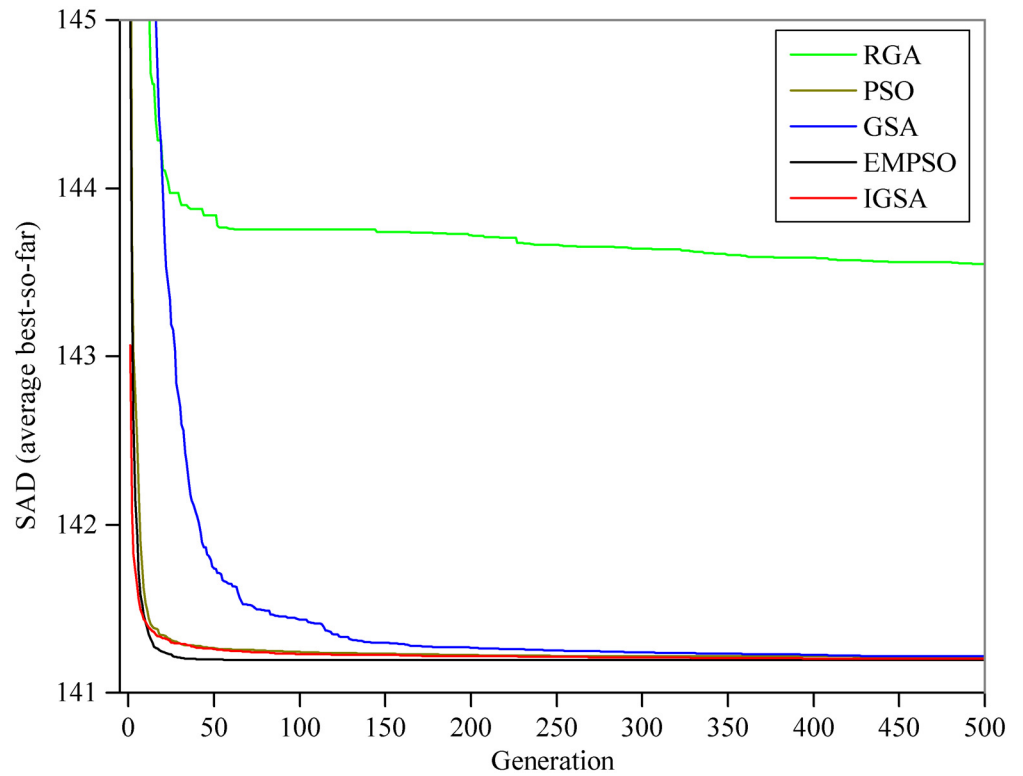


Fig 4. Average best curves for the LMM. All results represent the means of the 50 runs.

doi:10.1371/journal.pone.0147338.g004

Table 4. Statistics of different algorithms performed on the NLMM over 50 runs for the data set of Wilson (1974).

Algorithms	Statistics	<i>f</i>				Convergence ($\delta = 0.0001$)	
		SSQ	<i>K</i>	<i>x</i>	<i>m</i>	Iterations	CPU (s)
RGA	Best	36.7683	0.5184	0.2868	1.8677	3241	0.9613
	Worst	37.8397	0.6369	0.2881	1.8223	4548	1.3407
	Mean	36.9300	0.5266	0.2873	1.8646	1973	0.5888
	Std.	2.3267E-01	3.3579E-02	1.5334E-03	1.3702E-02	1844.47	5.4068E-01
PSO	Best	36.7691	0.5168	0.2871	1.8684	233	0.0536
	Worst	36.8376	0.5438	0.2875	1.8569	4390	0.9927
	Mean	36.7905	0.5162	0.2869	1.8687	2203	0.5007
	Std.	1.5596E-02	9.3849E-03	6.8361E-04	4.0096E-03	1453.70	3.2952E-01
GSA	Best	36.7694	0.5216	0.2870	1.8663	3022	1.5431
	Worst	38.0759	0.5514	0.2819	1.8555	40	0.0256
	Mean	37.0422	0.5492	0.2871	1.8553	2062	0.9992
	Std.	3.2174E-01	3.3700E-02	1.8361E-03	1.3696E-02	1669.06	7.9225E-01
EMPSO	Best	36.7679	0.5175	0.2869	1.8681	104	0.0475
	Worst	36.7679	0.5175	0.2869	1.8681	321	0.1450
	Mean	36.7679	0.5175	0.2869	1.8681	191	0.0883
	Std.	0.0000E+00	0.0000E+00	0.0000E+00	0.0000E+00	51.22	2.3747E-02
IGSA	Best	36.7679	0.5175	0.2869	1.8681	366	0.2332
	Worst	36.7679	0.5175	0.2869	1.8681	1051	0.6483
	Mean	36.7679	0.5175	0.2869	1.8681	780	0.4864
	Std.	0.0000E+00	0.0000E+00	0.0000E+00	0.0000E+00	119.17	7.1140E-02

doi:10.1371/journal.pone.0147338.t004

study is shown in Fig 5. Fig 6 shows the average convergence rate for the five different algorithms on the NLMM.

Case 2: Application to NLMM-L

River Wyre Flood in October 1982. The River Wyre flood event in October 1982 [21], which exhibits a considerable increase of flood volume (lateral flow) between the inflow section and the outflow section (approximately 25km), is selected as the numerical case for the NLMM-L. The flood data have multi-peaked inflow, in which $\Delta t = 1h$ and $T = 31$, and a major lateral flow contribution (which implies a large value of α). The search ranges for the four parameters in the NLMM-L are set to $K \in [0.01, 6.00]$, $x \in [0.00, 0.30]$, $m \in [0.50, 3.00]$ and $\alpha \in [0.00, 3.00]$. The best existing solution by the cuckoo search (CS) algorithm for the NLMM-L according to the literature [18] is $K = 5.6765$, $x = 0.2271$, $m = 0.9800$, $\alpha = 2.5298$ and $SSQ = 53.6574$.

Results and Analysis. For this numerical case to the NLMM-L, statistical results resemble Table 3 are presented in Table 5. As shown in Table 5: (1) only the EMPSO and IGSA can steadily find the global optimal solution in every run (the values of Std. for the SSQs and the parameters are 0.0000E+00), which is same to the reference; (2) the EMPSO still has the best performance in optimizing the NLMM-L (the lowest average CPU time for every run and a fairly steady fluctuation among iterations with the lowest Std. = 39.82). The estimated outflow hydrograph by the NLMM-L using the best solution obtained in this study is shown in Fig 7. Fig 8 shows the average convergence rate between the five different algorithms on the NLMM-L.

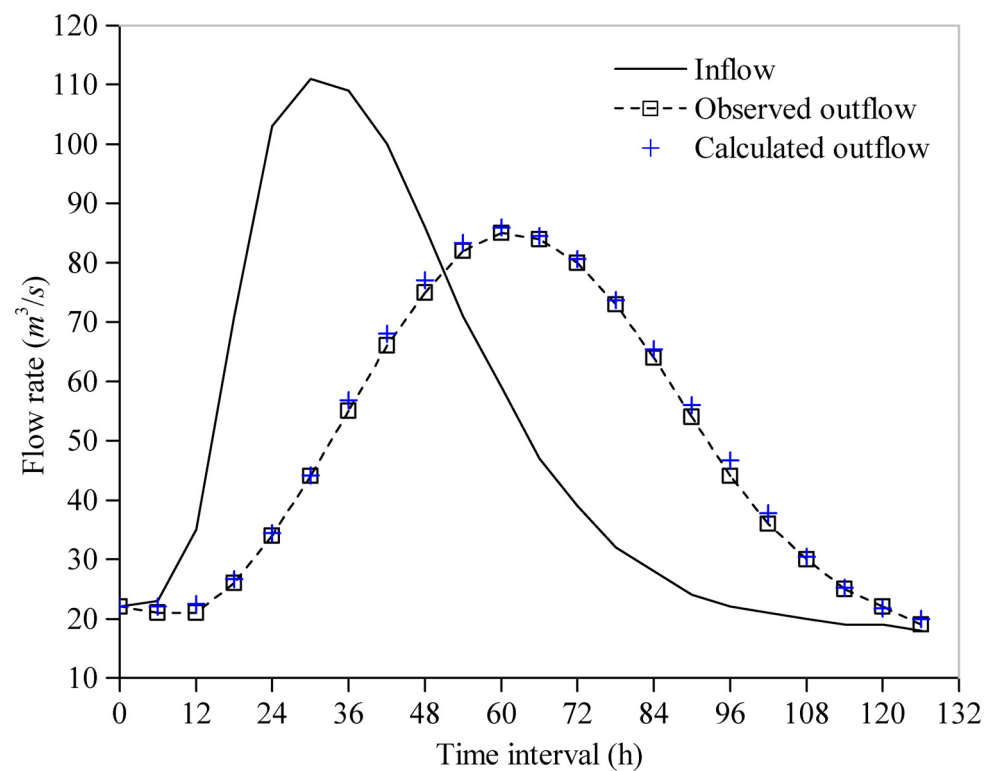


Fig 5. Fitting curve of outflow hydrograph of the NLMM experiment.

doi:10.1371/journal.pone.0147338.g005

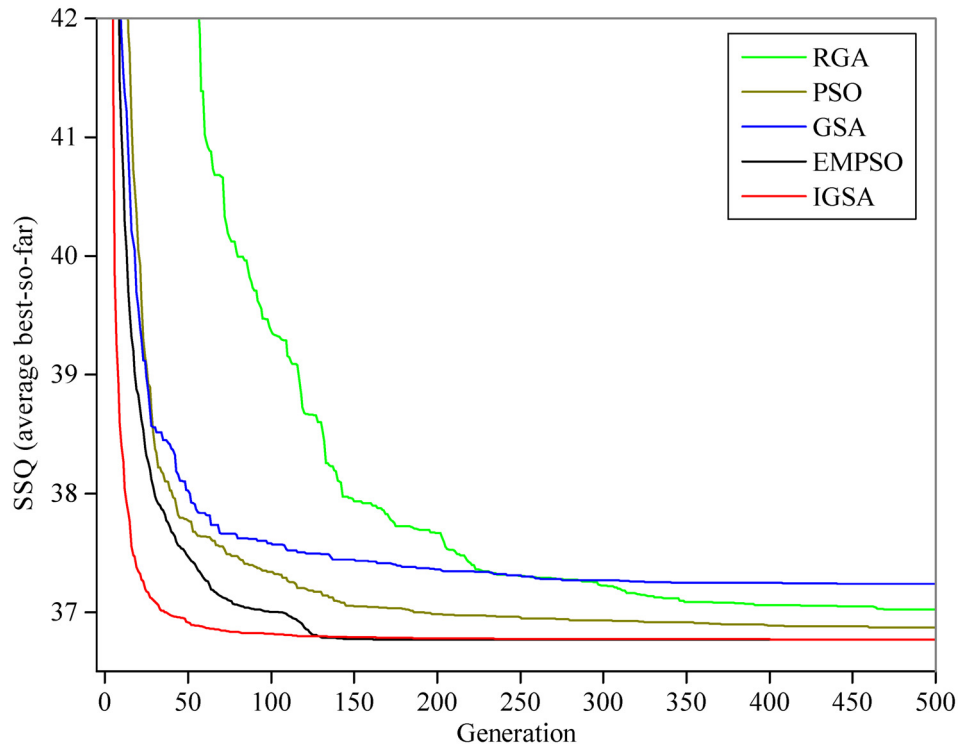


Fig 6. Average best curves for the NLMM.

doi:10.1371/journal.pone.0147338.g006

Table 5. Statistics of different algorithms performed on the NLMM-L over 50 runs for the River Wyre flood in October 1982.

Algorithms	Statistics	<i>f</i>					<i>P</i>		Convergence ($\delta = 0.0001$)	
		SSQ	<i>K</i>	<i>x</i>	<i>m</i>	α	Iterations	CPU (s)		
RGA	Best	53.8173	5.6300	0.2299	0.9821	2.5373	632	0.2863		
	Worst	66.9455	4.1086	0.2332	1.0470	2.5230	5000	2.0693		
	Mean	58.1929	4.8087	0.2310	1.0150	2.5253	4374	1.8169		
	Std.	3.5486E+00	3.6741E-01	1.9815E-03	1.6023E-02	2.6082E-03	1285.31	5.2463E-01		
PSO	Best	53.7213	5.7644	0.2258	0.9770	2.5319	3195	1.0745		
	Worst	56.0369	5.2233	0.2172	0.9960	2.5309	4903	1.6501		
	Mean	54.3777	5.6507	0.2277	0.9810	2.5307	2907	0.9797		
	Std.	4.9223E-01	2.1336E-01	4.6838E-03	7.7166E-03	4.7672E-03	1411.27	4.7516E-01		
GSA	Best	67.9146	4.0779	0.2294	1.0474	2.5204	145	0.1187		
	Worst	156.8379	2.2746	0.2342	1.1702	2.5148	4203	2.6463		
	Mean	101.8833	3.0891	0.2345	1.1070	2.5183	4178	2.6176		
	Std.	1.4658E+01	3.1027E-01	7.9331E-04	2.0579E-02	1.2428E-03	601.50	3.6447E-01		
EMPSO	Best	53.6574	5.6765	0.2271	0.9800	2.5298	131	0.0886		
	Worst	53.6574	5.6765	0.2271	0.9800	2.5298	298	0.2010		
	Mean	53.6574	5.6765	0.2271	0.9800	2.5298	196	0.1330		
	Std.	0.0000E+00	0.0000E+00	0.0000E+00	0.0000E+00	0.0000E+00	39.82	2.6695E-02		
IGSA	Best	53.6574	5.6765	0.2271	0.9800	2.5298	277	0.2386		
	Worst	53.6574	5.6765	0.2271	0.9800	2.5298	780	0.6520		
	Mean	53.6574	5.6765	0.2271	0.9800	2.5298	618	0.5201		
	Std.	0.0000E+00	0.0000E+00	0.0000E+00	0.0000E+00	0.0000E+00	97.18	7.9210E-02		

doi:10.1371/journal.pone.0147338.t005

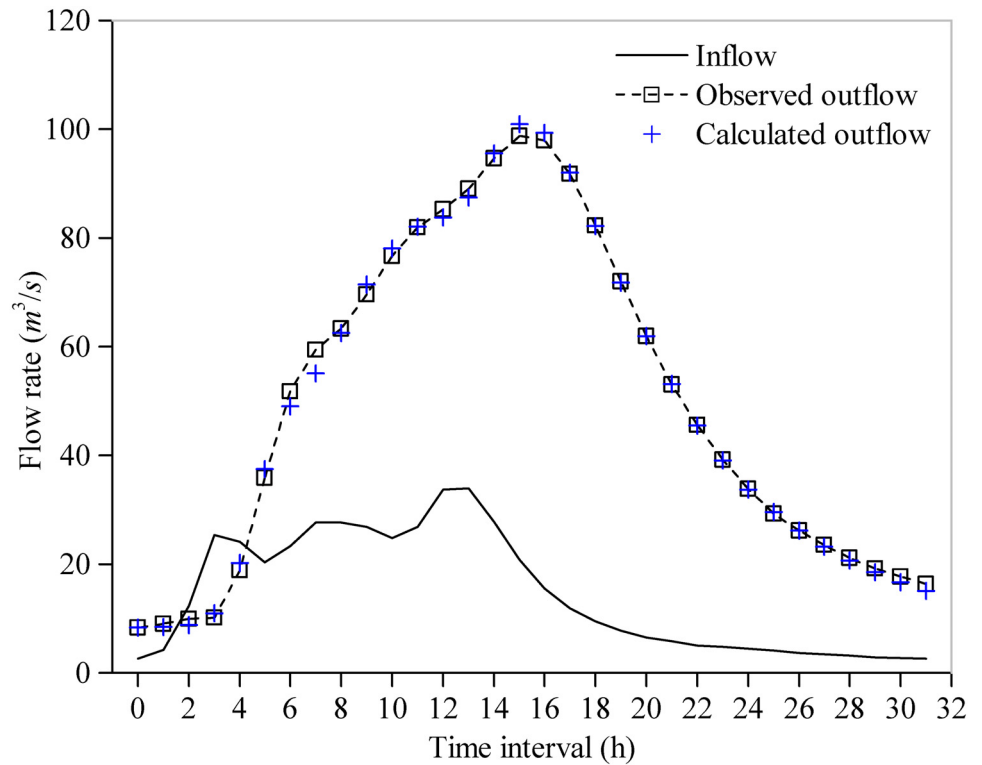


Fig 7. Fitting curve of outflow hydrograph of the NLMM-L experiment.

doi:10.1371/journal.pone.0147338.g007

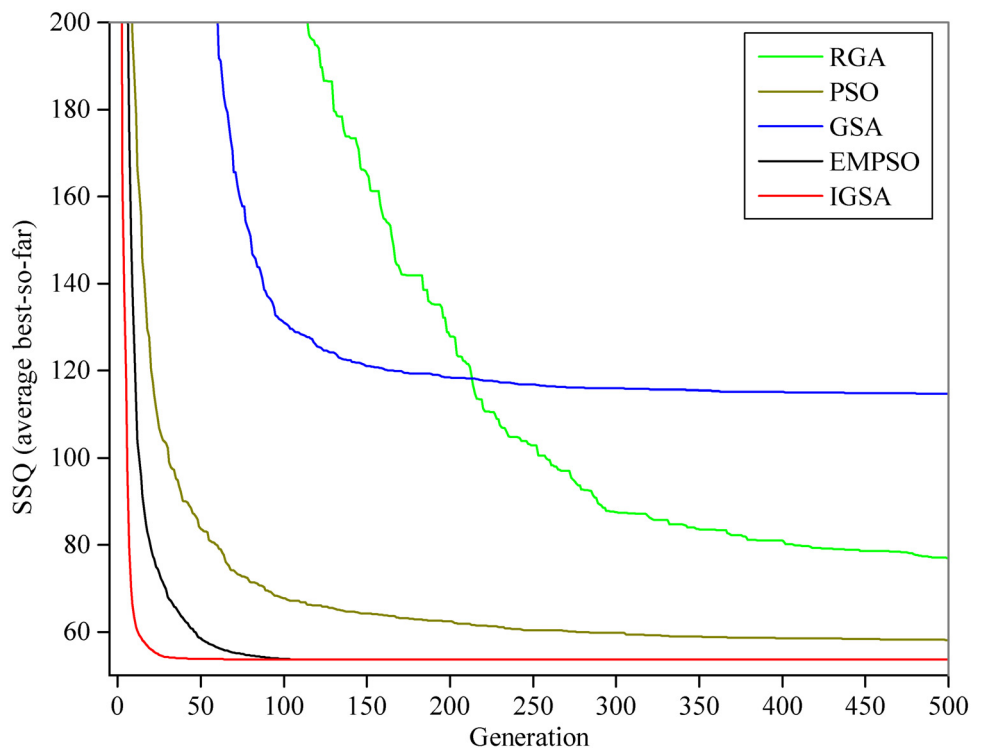


Fig 8. Average best curves for the NLMM-L.

doi:10.1371/journal.pone.0147338.g008

Conclusions

In this study, the EMPSO algorithm and the IGSA were applied for solving the parameter estimation problems of three forms of linear or nonlinear Muskingum models (LMM, NLMM and NLMM-L). The LMM has two parameters and the NLMM has three, whereas the NLMM-L considers the lateral flow along the river reach, which has a more complex structure with four parameters. The EMPSO and IGSA were tested on a rich set of 9 standard minimization benchmark functions. Then three typical flood events used in previous literature were selected as numerical cases (Case 1–3) to evaluate the practicability of the EMPSO and IGSA in applications. The results by the EMPSO and IGSA were compared with those obtained by the RGA, PSO and GSA, as well as the best reported solutions in the literature. Several conclusions are summarized as follows.

1. only the EMPSO and IGSA can steadily converge to the same optimal solution for the three Muskingum models in every run compared with RGA, standard PSO and the basic GSA;
2. the GSA may require more iterations and CPU time than the IGSA to find the same optimal solution for the LMM, and the results obtained by the GSA for the NLMM and the NLMM-L are the worst among the five algorithms (the largest values of SSQ and Std. in Tables 4 and 5), which indicates that the proposed IGSA can improve the performance (including the search efficiency, convergence speed and the stability) of GSA in optimizing the NLMM and the NLMM-L;
3. the EMPSO has the fastest convergence rate and the best robustness than the other four algorithms for the three Muskingum models in term of specified convergence accuracy and the Std. values.

Supporting Information

S1 Table. a_{ij} in function f8.

(DOCX)

S2 Table. Vectors a_i and c_i in function f9.

(DOCX)

S3 Table. Original data of each case and optimal estimated outflow hydrographs by the EMPSO and IGSA (m^3/s).

(DOCX)

Acknowledgments

This study was partly supported by the Hubei Support Plan of Science and Technology of China (No. 2015BCA291) and the Wuhan Planning Project of Science and Technology of China (No. 2014060101010062).

Author Contributions

Conceived and designed the experiments: LK SZ. Performed the experiments: SZ. Analyzed the data: LK SZ. Contributed reagents/materials/analysis tools: LK SZ. Wrote the paper: LK SZ.

References

1. Chow VT, Maidment DR, Mays LW. Applied hydrology. New York: McGraw-Hill; 1988.

2. Geem ZW. Issues in optimal parameter estimation for the nonlinear Muskingum flood routing model. *Engineering Optimization*. 2014; 46(3): 328–339.
3. McCarthy GT. The unit hydrograph and flood routing. Conference of North Atlantic Division; 1938.
4. Das A. Parameter Estimation for Muskingum Models. *Journal of Irrigation and Drainage Engineering*. 2004; 130(2): 140–147.
5. Gill MA. Flood routing by the Muskingum method. *Journal of Hydrology*. 1978; 36(3–4): 353–363.
6. Tung Y. River Flood Routing by Nonlinear Muskingum Method. *Journal of Hydraulic Engineering*. 1985; 111(12): 1447–1460.
7. Yoon J, Padmanabhan G. Parameter Estimation of Linear and Nonlinear Muskingum Models. *Journal of Water Resources Planning and Management*. 1993; 119(5): 600–610.
8. Geem ZW. Parameter Estimation for the Nonlinear Muskingum Model Using the BFGS Technique. *Journal of Irrigation and Drainage Engineering*. 2006; 132(5): 474–478.
9. Barati R. Parameter Estimation of Nonlinear Muskingum Models Using Nelder-Mead Simplex Algorithm. *Journal of Hydrologic Engineering*. 2011; 16(11): 946–954.
10. Kim JH, Geem ZW, Kim ES. Parameter Estimation of the Nonlinear Muskingum Model Using Harmony Search1. *JAWRA Journal of the American Water Resources Association*. 2001; 37(5): 1131–1138.
11. Chen J, Yang X. Optimal parameter estimation for Muskingum model based on Gray-encoded accelerating genetic algorithm. *Communications in Nonlinear Science and Numerical Simulation*. 2007; 12(5): 849–858.
12. Ma X, Shu D, Huang Y. Parameter Estimation Method of Nonlinear Muskingum Model Based on PSO. *Journal of Zhengzhou University (Engineering Science)*. 2007; 28(4): 122–125.
13. Yang Z, Kang L. Application and comparison of several intelligent algorithms on Muskingum Routing Model. *Proceedings of the 2nd IEEE International Conference on Information and Financial Engineering (ICIFE)*. 2010: 910–914.
14. Chu H, Chang L. Applying Particle Swarm Optimization to Parameter Estimation of the Nonlinear Muskingum Model. *Journal of Hydrologic Engineering*. 2009; 14(9): 1024–1027.
15. Ouyang A, Li K, Truong TK, Sallam A, Sha EH-M. Hybrid particle swarm optimization for parameter estimation of Muskingum model. *Neural Computing and Applications*. 2014; 25(7–8): 1785–1799.
16. Luo J, Xie J. Parameter Estimation for Nonlinear Muskingum Model Based on Immune Clonal Selection Algorithm. *Journal of Hydrologic Engineering*. 2010; 15(10): 844–851.
17. Xu D, Qiu L, Chen S. Estimation of Nonlinear Muskingum Model Parameter Using Differential Evolution. *Journal of Hydrologic Engineering*. 2012; 17(2): 348–353.
18. Karahan H, Gurarslan G, Geem ZW. A new nonlinear Muskingum flood routing model incorporating lateral flow. *Engineering Optimization*. 2014; 47(6): 737–749.
19. Nagesh Kumar D, Janga Reddy M. Multipurpose reservoir operation using particle swarm optimization. *Journal of Water Resources Planning and Management*. 2007; 133(3): 192–201.
20. Rashedi E, Nezamabadi-pour H, Saryazdi S. GSA: A Gravitational Search Algorithm. *Information Sciences*. 2009; 179(13): 2232–2248.
21. O'Donnell T. A direct three-parameter Muskingum procedure incorporating lateral inflow. *Hydrological Sciences Journal*. 1985; 30(4): 479–496.
22. Kennedy J, Eberhart R. Particle swarm optimization. *Proceedings of the 1995 IEEE International Conference on Neural Networks*. 1995: 1942–1948.
23. Clerc M. The swarm and the queen: towards a deterministic and adaptive particle swarm optimization. *Proceedings of the 1999 Congress on Evolutionary Computation*. 1999: 1951–1957.
24. Gao Y, Du W, Yan G. Selectively-informed particle swarm optimization. *Scientific Reports*. 2015; 5: 9295. doi: [10.1038/srep09295](https://doi.org/10.1038/srep09295) PMID: [25787315](https://pubmed.ncbi.nlm.nih.gov/25787315/)
25. Liu C, Du W-B, Wang W-X. Particle Swarm Optimization with Scale-Free Interactions. *Plos One*. 2014; 9(5): e97822. doi: [10.1371/journal.pone.0097822](https://doi.org/10.1371/journal.pone.0097822) PMID: [24859007](https://pubmed.ncbi.nlm.nih.gov/24859007/)
26. Shi Y, Eberhart R. A modified particle swarm optimizer. *The 1998 IEEE International Conference on Evolutionary Computation Proceedings*. 1998: 69–73.
27. Kennedy J, Mendes R. Population structure and particle swarm performance. *Proceedings of the 2002 Congress on Evolutionary Computation*. 2002: 1671–1676.
28. Li C, Yang S. An adaptive learning particle swarm optimizer for function optimization. *Proceedings of the 2009 IEEE Congress on Evolutionary Computation*. 2009: 381–388.
29. Mendes R, Kennedy J, Neves J. The fully informed particle swarm: simpler, maybe better. *IEEE Transactions On Evolutionary Computation*. 2004; 8(3): 204–210.

30. Du W-B, Gao Y, Liu C, Zheng Z, Wang Z. Adequate is better: particle swarm optimization with limited-information. *Applied Mathematics and Computation*. 2015; 268: 832–838.
31. Mirjalili S, Hashim SZM. A new hybrid PSO-GSA algorithm for function optimization. *Proceedings of 2010 International Conference on Computer and Information Application (ICCIA 2010)*. 2010: 374–377.
32. Wang G-G, Gandomi AH, Yang X-S, Alavi AH. A novel improved accelerated particle swarm optimization algorithm for global numerical optimization. *Engineering Computations*. 2014; 31(7): 1198–1220.
33. Jamil M, Yang X-S. A literature survey of benchmark functions for global optimisation problems. *International Journal of Mathematical Modelling and Numerical Optimisation*. 2013; 4(2): 150–194.
34. Vesterstrom J, Thomsen R. A comparative study of differential evolution, particle swarm optimization, and evolutionary algorithms on numerical benchmark problems. *Proceedings of 2004 Congress on Evolutionary Computation*. 2004: 1980–1987.
35. Deb K. An efficient constraint handling method for genetic algorithms. *Computer Methods in Applied Mechanics and Engineering*. 2000; 186(2–4): 311–338.
36. Qu GJ. Parameter estimation for Muskingum models. *Journal of Hydrology*. 1977; 36(3): 40–43.
37. Wilson EM. *Engineering Hydrology*. London, England: Macmillan Book Company; 1974.
38. Al-Humoud JM, Esen II. Approximate Methods for the Estimation of Muskingum Flood Routing Parameters. *Water Resources Management*. 2006; 20(6): 979–990.

© 2016 Kang, Zhang. This is an open access article distributed under the terms of the Creative Commons Attribution License:

<http://creativecommons.org/licenses/by/4.0/> (the “License”), which permits unrestricted use, distribution, and reproduction in any medium, provided the original author and source are credited. Notwithstanding the ProQuest Terms and Conditions, you may use this content in accordance with the terms of the License.